JOURNAL OF IMAGING SCIENCE AND TECHNOLOGY • Volume 43, Number 6, November/December 1999

Physical Characterization of Silver Behenate as a Tool for the Development of Thermographic and Photothermographic Materials

Ingrid Geuens
Agfa-Gevaert NV Mortsel, Belgium

Iris Vanwelkenhuysen
University of Antwerp, Belgium

Silver behenate is used in thermographic materials as the image silver reservoir. To obtain an imaging material with optimal sensitometric and physical properties, it is important to obtain fundamental insight into and basic knowledge of silver behenate. A method for determining the relative crystallinity has been developed based on powder x-ray diffraction (XRD). In addition, the thermal behavior of silver behenate crystals has been studied using XRD. The image silver crystal size, silver behenate crystallinity and phase transitions were determined at different temperatures.

Journal of Imaging Science and Technology 43: 521–527 (1999)

Introduction

In order to understand the mechanism and optimize the performance of thermographic and photothermographic materials it is important to get some insight in the components of the materials. Silver behenate is one of the organic silver salts used in thermographic and photothermographic materials as a silver reservoir for image formation.[1–3] With x-ray diffraction analysis it is possible to determine the crystal structure of silver behenate and variations thereof.[4–6] The presence of phase transitions during temperature treatment, the crystallinity and the incorporation of elements and species can be determined by XRD.[7,8] The crystal sizes of the metallic silver forming during and after the development reaction are also quantified.

Experimental

X-ray diffractometers from Siemens (D500) and Philips (X'PERT-MPD) were used in this study. A CuKα (0.1542 nm) x-ray tube at 30 mA current and 40keV energy using different apertures, detector diaphragms, step sizes (0.050°-0.018°) and acquisition times per step (1–10s), depending on the application, were utilized. The samples were spun during the measurement. The spinning time was changed according to the step size used. The XRD measurements were all performed directly on coated film material.[9] For the quantitative analysis, the influence of silver behenate coating thickness was eliminated by normalizing using the Ag concentration as measured by x-ray fluorescence. The influence of other factors was minimal and does not affect the XRD analysis.

TEM measurements were obtained on a Philips CM200 instrument, at 120kV accelerating voltage.

Results and Discussion

Silver behenate can differ in size, morphology and shape depending on the synthesis conditions, as can be seen in Fig. 1. The morphology can vary from an elongated spiral form more than 10μm long to flat microcrystals of only 1 μm or less.

Crystallinity of Silver Behenate. Another property of silver behenate is its crystallinity which can also be varied by varying its synthesis conditions.[9] X-ray diffraction analysis offers the possibility of determining the crystallinity quantitatively.

Differences in crystallinity were observed in XRD spectra as changes in the overall intensity of all silver behenate diffraction peaks (Fig. 2). A method was developed to determine the relative crystallinity directly in the film material.[9]

Method Development

Using six diffraction peaks of silver behenate, those at $2\theta = 6.01°$, 7.56°, 9.12°, 10.66° and 12.12°, the integral peak height of these six diffraction peaks, K was calculated. This value was corrected for instrument dependence by normalizing with the integral peak height of a NIST standard 1976 Al_2O_3 (JCPDS 42-1468) at $2\theta =$ 25.60°, 35.16° and 43.40°. K_r is thus calculated as $K_r = \sum I_j$ with I the peak height at the corresponding positions j = (012), (104), (113).

The intensity of diffraction peaks is not only dependent on the crystallinity of the material, but also on the amount of material present. In order to eliminate dependence upon the amount of Ag in the material, the

---

Original manuscript received April 5, 1999

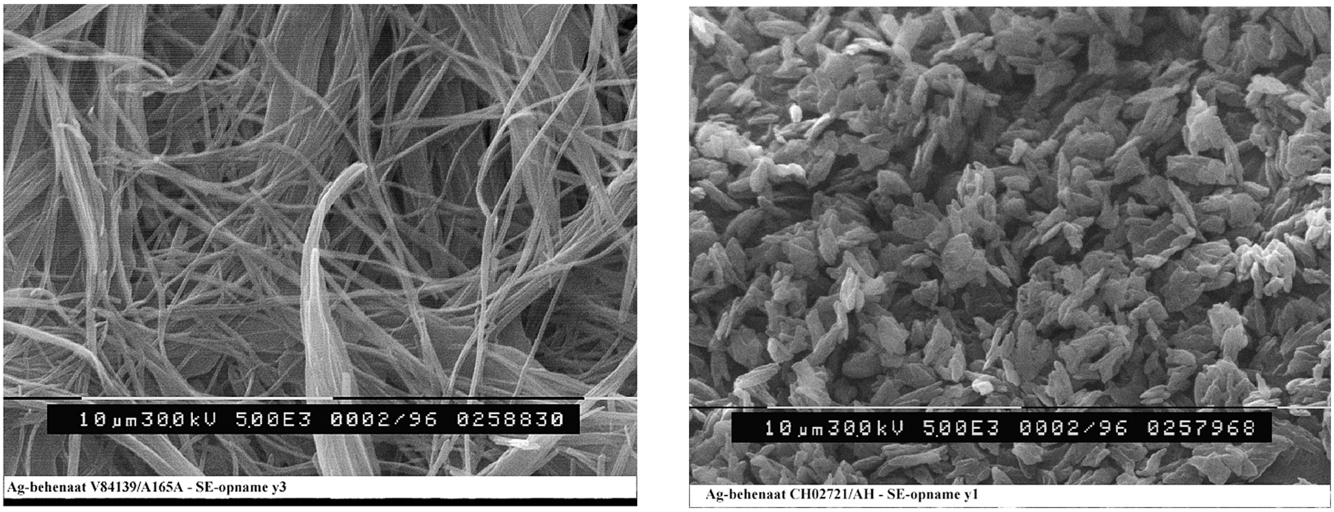

(a) (b)

Figure 1. Secondary electron images of silver behenate at a magnification of 5000x.

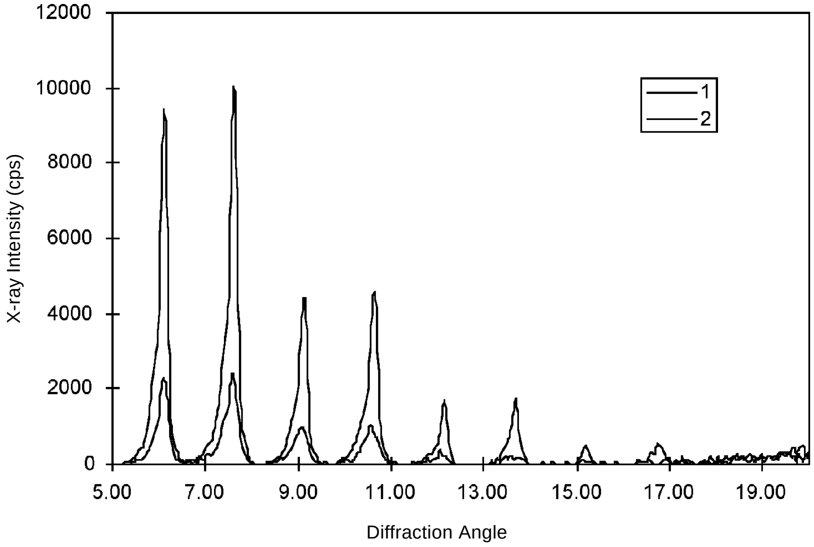

Figure 2. X-ray diffraction spectral of different types of silver behante. The overall x-ray intensity is much smaller for type 1 crystals, corresponding to the silver behenate in Fig. 1a.

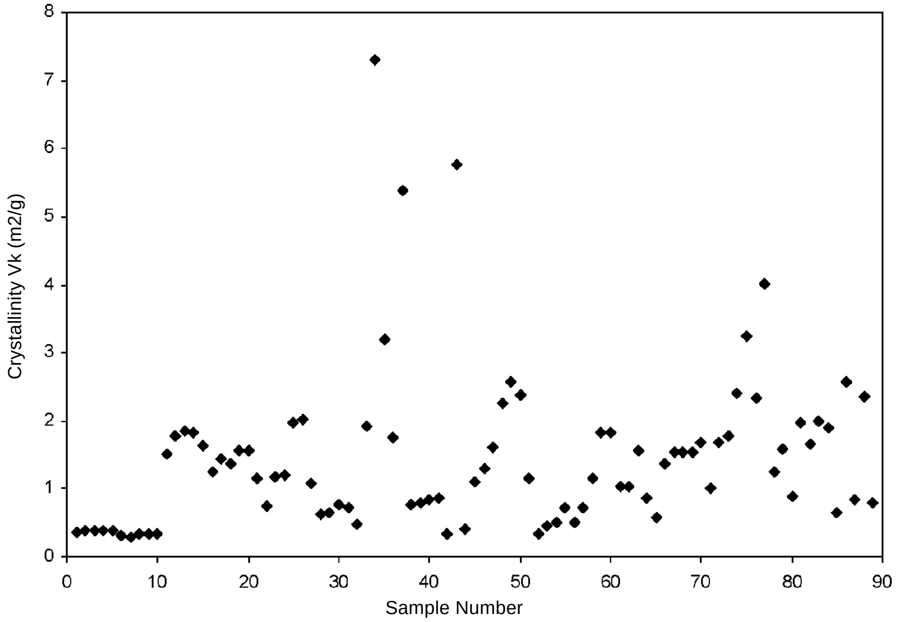

Figure 3. Examples of measured relative silver behenate crystallinities.

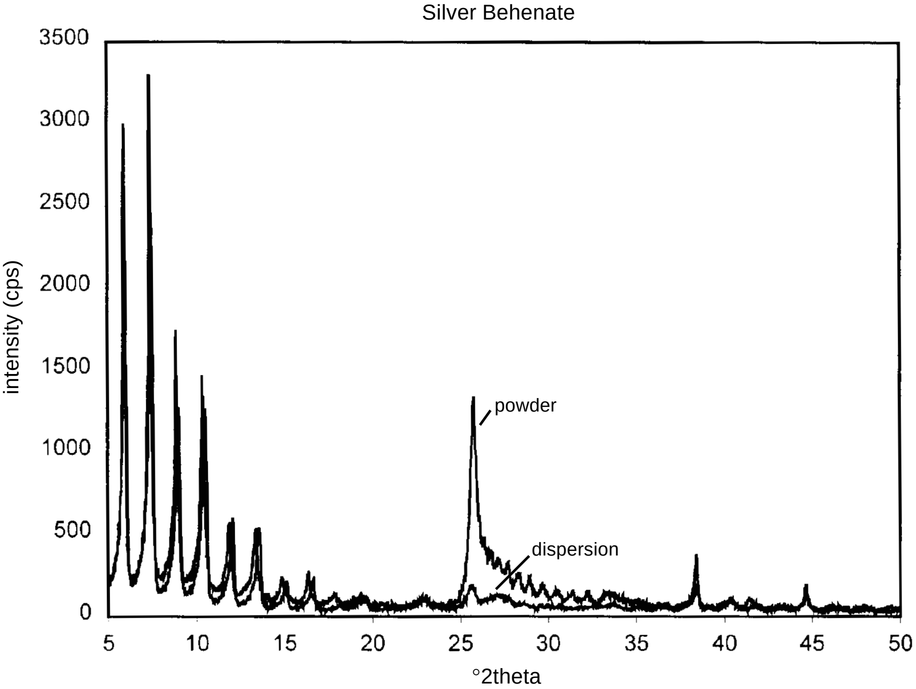

Figure 4. XRD spectra of a powder and a dispersion of silver behenate: small distances are lost and the overall crystallinity is decreased.

ratio K/K_r is divided by the silver concentration C_{Ag}, so that a relative crystallinity V_k can be obtained where $V_k = K/(K_r * C_{Ag})$. The Ag concentration was measured with wavelength dispersive x-ray fluorescence and is expressed in g/m^2. The Ag concentration can be measured with a precision of 0.2%. Orientation of the crystals can also influence the overall crystallinity. Spinning removes the variability of in-plane orientation, therefore the samples are spun during measurement in order to obtain the mean orientation. However, the difference in orientations of in-plane versus out-of-plane has not been corrected for. By carefully examining the overall XRD spectrum, it was seen that all the diffraction peaks were changed equally. Different commercially available samples were analyzed and compared. By making sections of the different film materials and observing the orientation of the individual silver behenate crystals, with electron microscopy, it was concluded that no effect of the difference in orientation of in-plane versus out-of-plane was observed. The effect of the in-plane orientation was observed only if no spinning was used. The precision of the measurement of the relative crystallinity by this technique, V_k is 6.5% at the 95% confidence level.

Examples of Crystallinity Measured on Film Material

The crystallinity of silver behenate is influenced by its synthesis conditions, how it is dispersed and coated and by other components within the coating composition. Figure 3 gives an idea of the variations observed in the relative crystallinity obtained over a large collection of silver behenate samples. Differences in XRD diffraction peak ratios are also found when powders are compared with dispersions. The observed pattern is dramatically affected and it can be seen that the small distances are lost once the powder is dispersed and coated (Fig. 4). Orientation can influence these intensity ratios, although when a dispersion is dried as a droplet with an intended drastic difference in the orientation of the crystals, the same effects were observed. Therefore, only crystallinities of coated materials were compared. For coated materials the relative crystallinity has been found to vary between 0.3 and 7 m^2/g.

When silver halide is present in photothermographic material, the crystal structure and crystallinity of the silver behenate can be influenced. Figure 5 shows an example of the effect of iodide conversion growth on the silver behenate crystallinity. If an iodide conversion growth is performed, the crystallinity is increased, regardless of the synthesis conditions used for the silver behenate. Adding AgBr, after the iodide conversion growth, results first in an increase in the relative AgBr (100) peak intensity. Additional AgBr results in a reduced AgBr (100) peak intensity and a decrease of the AgI x-ray diffraction peaks. At the same time a shift of the AgBr (100) peak is observed. Addition of AgBr resulted in Ag(Br,I) crystal formation (Fig. 6).

Metallic Silver Crystal Size. The mean silver crystal size can be determined from the XRD spectra of thermally processed material, due to the fact that there is an inverse relationship between the crystal size and the diffraction peak broadening for crystals of 1 up to at least 100 nm.

Method Development

The mean silver size of crystallites can be determined using the well known Scherrer formula.[10]

$$D = K\lambda/[\cos\theta(\beta-\beta_s)]$$

where D is the crystallite size (nm), K, a form factor (no dimension), λ, the wavelength of the incident x-rays (CuKα =0.1542 nm), β, the full width at half maximum of the diffraction peak (in rad), β_s the full width at half maximum originating from the instrument and θ is the peak position (in rad).

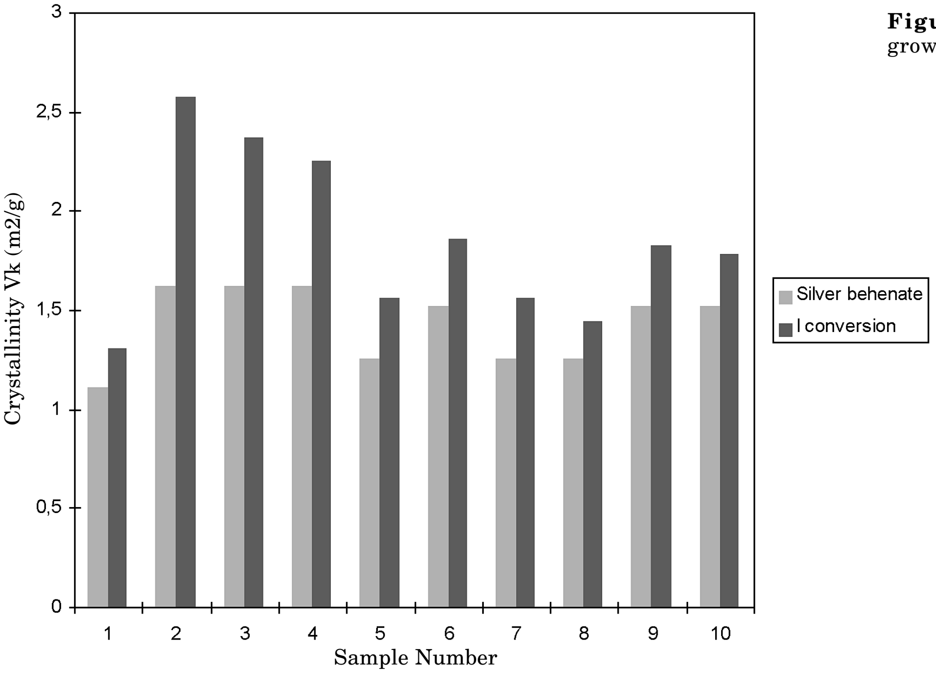

Figure 5. Effect of iodide conversion growth on the relative crystallinity.

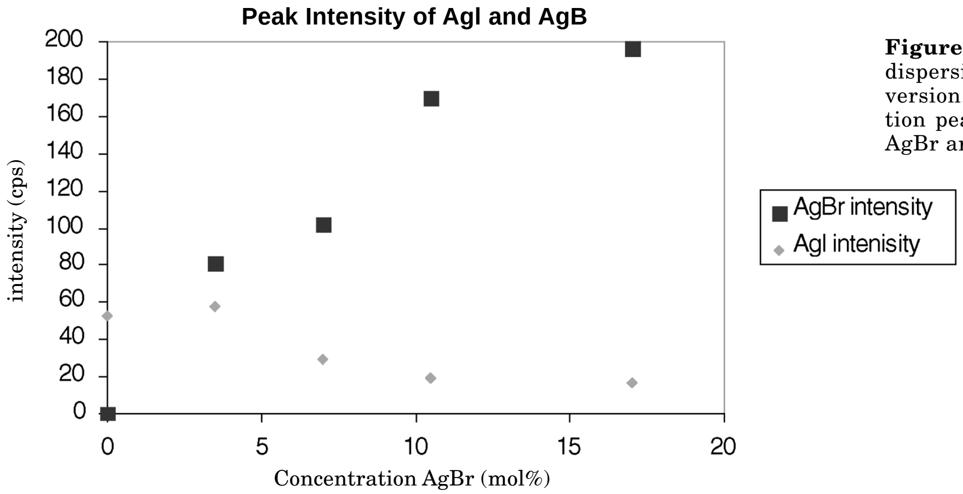

Figure 6. The effect of adding AgBr to a dispersion of Ag behenate with iodide conversion. The x-ray intensity of the diffraction peaks of the (100) phases of AgI and AgBr are provided.

$\theta = 0.3329$ rad was used for the determining the silver crystallite size (Fig. 7). The broadening caused by the instrument was corrected for by measuring a 111-crystal of AgBr. The peak broadening due to the instrument was 0.12°. The crystal size can be measured perpendicular to a certain plane or the mean crystal size is determined by calculating the size for all planes. It was found using transmission electron microscopy that the silver crystallites were generally more or less spherical. For spherical crystallites, the mean crystal size therefore equals the size perpendicular towards any given plane. A form factor of 0.95 was used for the mean size. If the crystallite form was not known in advance, a form factor of 0.90 was used for the size determination perpendicular to the (111) face. The choice of the form factor was based upon the results known on crystals for which the shape was not known in advance.[10]

The mean dimensions of the silver crystallites, perpendicular to the (111) face, were reproducible within 3%. The accuracy was checked with transmission electron microscope images. The measured size in the TEM images for single crystals was in good agreement with that found using XRD spectra.

Examples of Metallic Silver Size Determination in Processed Thermo- and Photothermographic Materials. The mean Ag crystallite size was found to vary over a very small range, between 4 and 20 nm. Photothermographic materials form larger Ag crystal sizes: between 14 to 20nm.[3,11,12] The size of the Ag crystallites in thermally processed materials were found to depend upon the processing conditions, the presence of a coating layer and the coating composition. Figure 8 evaluates the dimension of Ag crystallites determined in a large collection of different processed materials. Processing conditions such as time and temperature can change the Ag crystal size depending on the type of silver behenate used. Figure 9 shows the effect of adding a coating layer. When a topcoat is present on top of the emulsion layer the silver crystal size is observed to be affected. Also the method of coating the material can influence the metallic silver

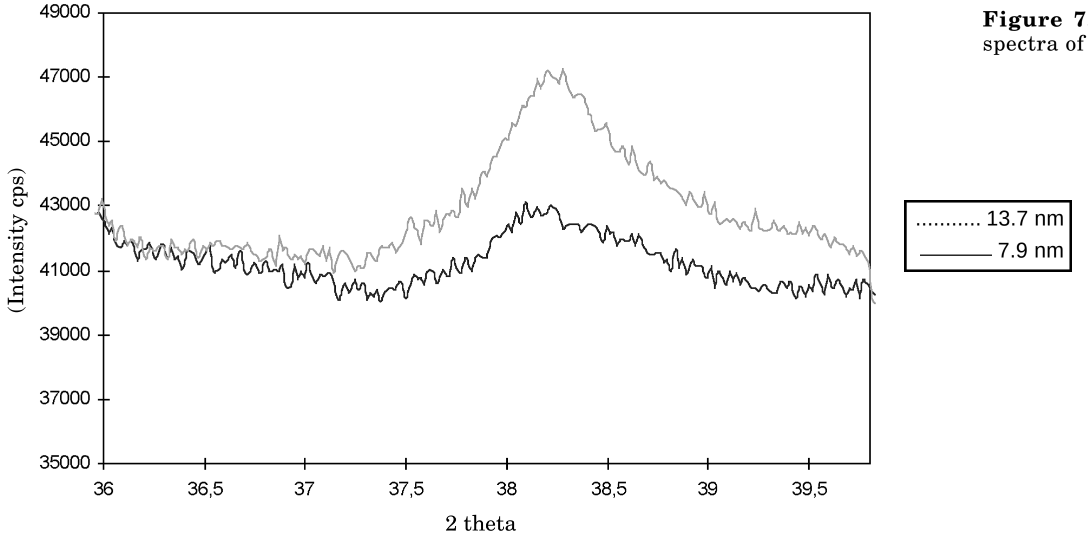

Figure 7. A detail of the XRD spectra of the Ag^0 (111) plane.

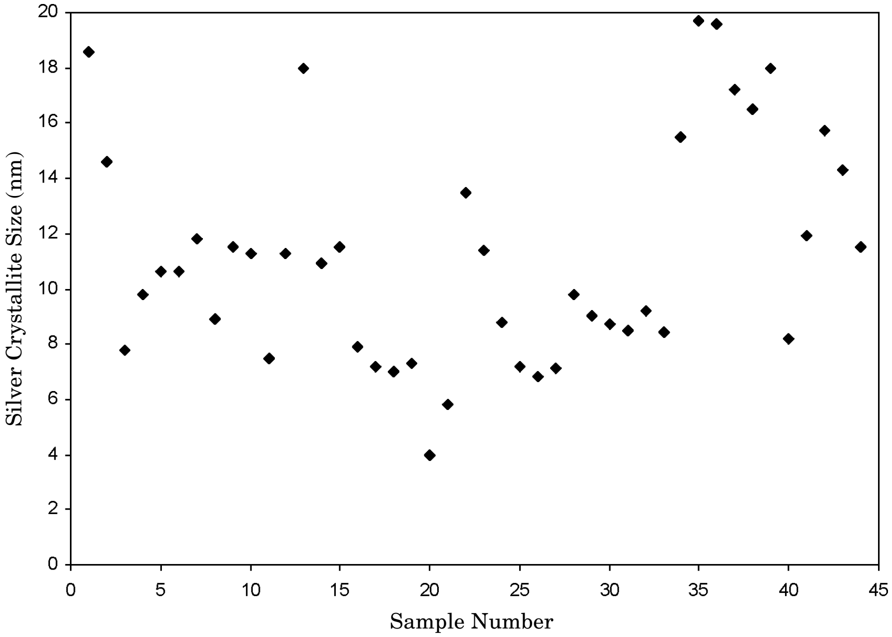

Figure 8. Examples of measured silver crystallite sizes.

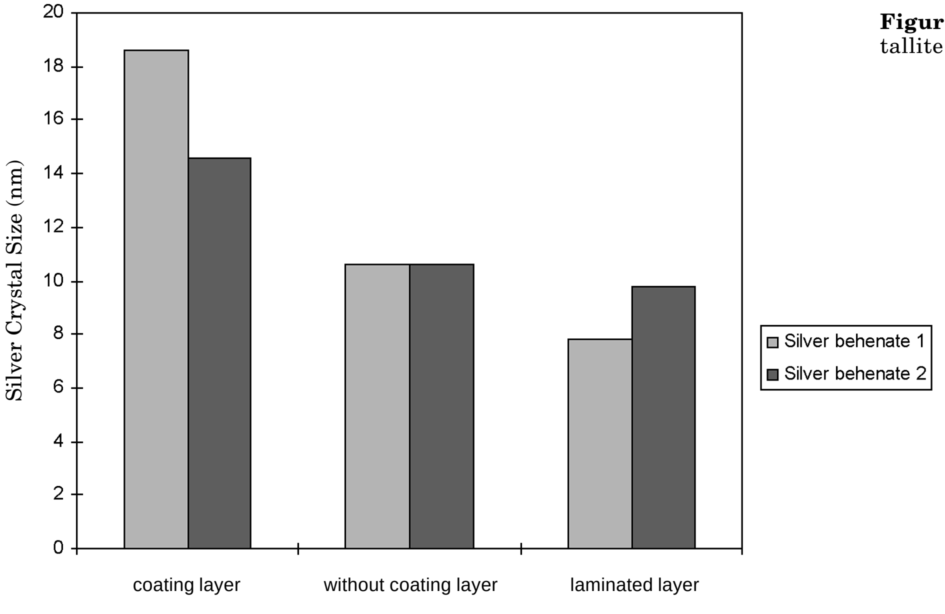

Figure 9. Effect of topcoat on the silver crystallite size in an imaging film construction.

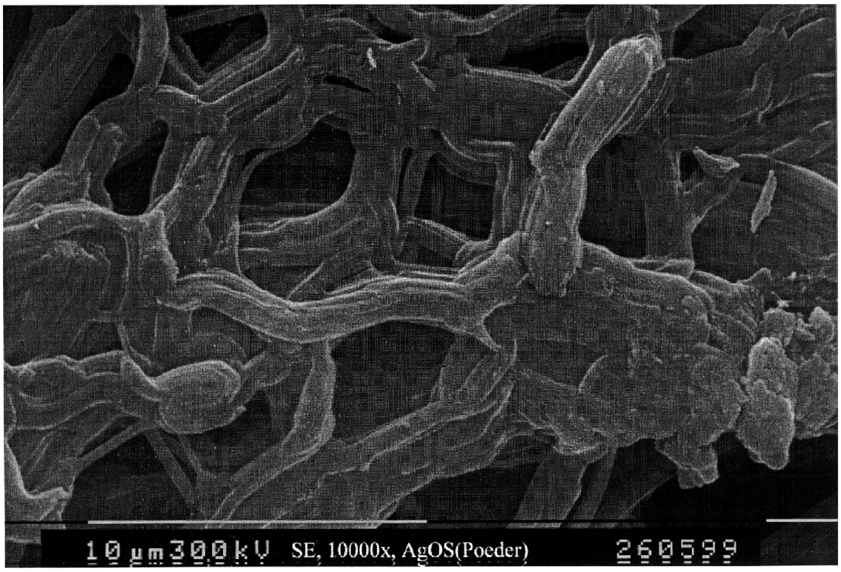

Figure 10. Secondary electron image of silver behenate heated up to 150°C at a magnification of 10,000x.

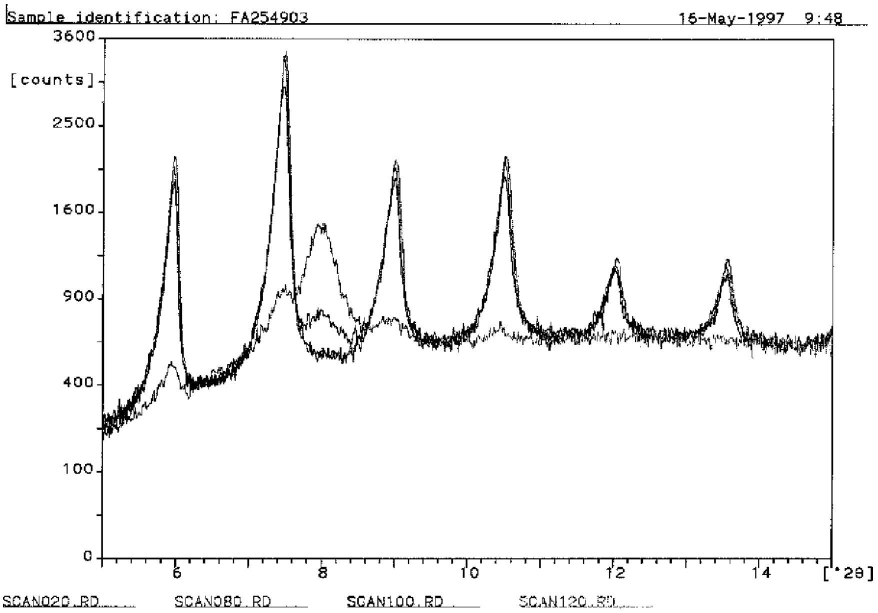

Figure 11. The behavior of the silver behenate during in situ temperature experiments at 20°C, 80°C, 100°C and 120°C.

crystallite size. The mean crystal size of 4 to 20nm cannot explain the image performance. It was found that not only the size of the crystals is important for the image performance but also their spatial distribution.

Thermal Behavior of Silver Behenate

Ex situ experiments were carried out on silver behenate containing layers. The samples of film material were heated to 100°C, 120°C, 150°C and 200°C and then cooled. XRD measurements were performed at room temperature. The silver behenate is stable up to 120°C. Neither loss of crystallinity nor decomposition was observable. Treatment at higher temperatures resulted in a decrease in silver behenate diffraction peak intensity. At 200°C, silver and behenic acid were present. The morphology also changes drastically above 150°C (Fig. 10).

The XRD of silver behenate was also investigated in situ during temperature treatment. The material was heated at 20°C, 80°C, 100°C, 120°C, 130°C, 140°C, 150°C and 200°C during which the XRD spectra were recorded using a position sensitive detector. Up to 100°C, the silver behenate was stable. At higher temperatures a new phase becomes visible in the XRD spectra and there is a loss of crystallinity of the silver behenate (Fig. 11). Neither metallic silver nor behenic acid was detected. At 120 and 130°C the new phase of silver behenate becomes dominant and the original crystal structure disappears (Fig. 12).[8] At 140°C only amorphous silver behenate was present. This is visualized in a scanning electron microscope as a melting phase (Fig. 10). Up to 150°C neither metallic silver nor behenic acid could be detected.

When coated material is heated for several minutes, a loss of crystallinity can also be detected at 100°C after 90 min. The crystallinity, V_k, as defined above, sometimes decreased by more than half (Fig. 13).

Conclusions

With X-ray diffraction it is possible to characterize quantitatively the crystallinity of the silver behenate and to determine the size of the metallic silver crystal present in the processed film materials. Silver behenate

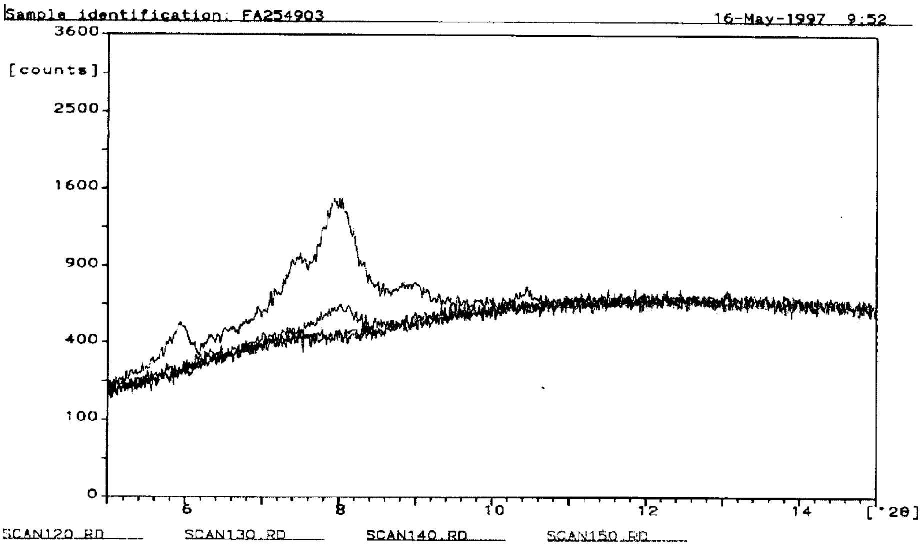

Figure 12. The behavior of the silver behenate during in situ temperature experiments at 120°C, 130°C, 140°C, and 150°C.

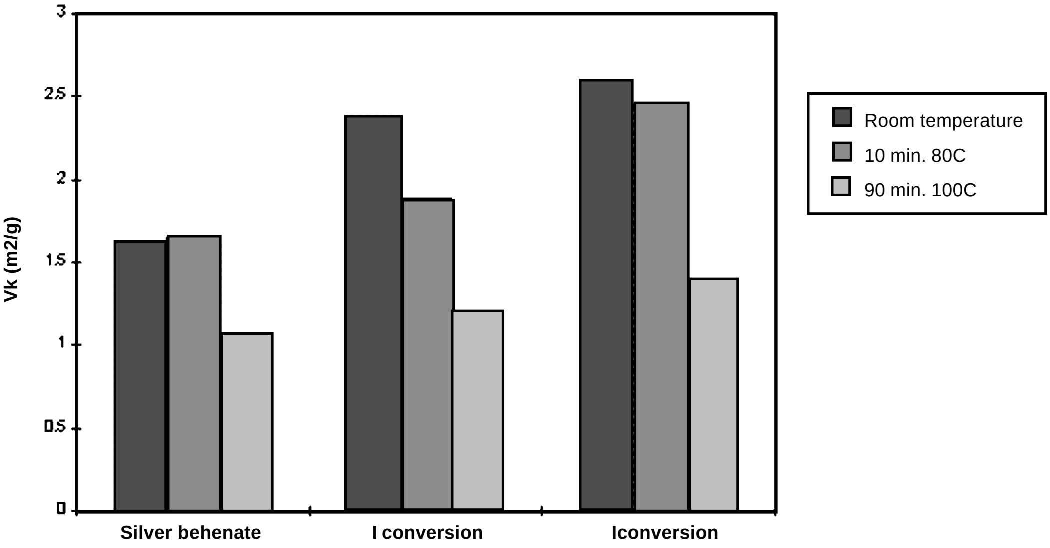

Figure 13. Effect of extended heating on silver behenate crystallinity.

crystallinity was found to range from 0.3 to 7m^2/g. In addition, the thermal behavior of the silver behenate can also be characterized. Under temperature treatment the silver behenate can be observed to undergo several transitions.

References

1. M. R. V. Sahyun, *J. Imaging Sci. Technol.* **42,** 23 (1998).
2. E. K. Fields, *J. Org. Chem.* **41,** 916 (1976).
3. B. B. Bokhonov and L. P. Burleva, *J. Imaging Sci. Technol.* **40**, 417 (1996).
4. T. C. Huang, H. Toraya, T. N. Blanton, and Y. Wu, *J. Appl. Cryst.* **26,** 180 (1993).
5. T. N. Blanton, T. C. Huang, H. Toraya, C. R. Hubbard, S. B. Robie, D. Louer, H. E. Gobel, G. Will, R. Gilles, and T. Raftery, *Powder Diffr.* **10,** 91 (1995).
6. V. Vand, A. Aitken and R. K. Campbell, *Acta. Cryst.* **2,** 398 (1949); B. P. Tolochko, S. V. Chernov, S. G. Nikitenko, and D. R. Whitcomb, *Nucl. Instr. Meth. Phys. Res. (A)* **405,** 428 (1998).
7. M. Ikeda and Y. Iwata, *Photogr. Sci. Eng.* **24,** 273 (1980).
8. M. Ikeda, *Photogr. Sci. Eng.* **24,** 277 (1980).
9. B. Horsten, I. Geuens, Y. Gilliams, A. Bellens, D. Bollen, and I. Hoogmartens, EP 848,286 (1997).
10. H. P. Klug and L. E. Alexander, Wiley, *X-ray Diffraction Procedures* (1954).
11. B. B. Bokhonov and L. P. Burleva, *J. Imaging Sci. Technol.* **40,** 85 (1996).
12. S. E. Hill, M. B. Mizen and M. R. V. Sayhun, *J. Imaging Sci. Technol.* **40,** 568 (1996).